

## Selected Aspects of 3D Printing for Emergency Replacement of Structural Elements

Krzysztof Jasiński<sup>1</sup>, Lech Murawski<sup>2</sup>, Marcin Kluczyk<sup>3</sup>, Adam Muc<sup>1\*</sup>, Adam Szeleziński<sup>2</sup>, Tomasz Muchowski<sup>2</sup>, Marek Chodnicki<sup>4</sup>

<sup>1</sup> Faculty of Electrical Engineering, Gdynia Maritime University, ul. Morska 81-87, 81-225 Gdynia, Poland

<sup>2</sup> Faculty of Maritime Engineering, Gdynia Maritime University, ul. Morska 81-87, 81-225 Gdynia, Poland

<sup>3</sup> Mechanical-Electrical Faculty, Polish Naval Academy, ul. Śmidowicza 69, 81-127 Gdynia, Poland

<sup>4</sup> Faculty of Mechanical Engineering and Ship Technology, Gdańsk University of Technology, ul. Gabriela Narutowicza 11/12, 80-233 Gdańsk, Poland

\* Corresponding author's e-mail: a.muc@we.umg.edu.pl

### ABSTRACT

The paper presents a synthetic characterization of modern methods of manufacturing or regenerating machine elements. Considered methods are machining and additive methods, in particular 3D printing in the FDM/FFF technique. For the study, the authors made samples of the holder bracket using selected methods. Samples made by machining operations, 3D printing with various filling were tested. The paper contains a technical and economic analysis of the production of a holder bracket using the discussed methods. The dynamics of steel and FDM/FFF printed samples were also assessed by determining their resonance curves. The vibration magnification factors were analyzed – the quotient of the vibration amplitudes in the resonance to the static deformations that occurred under the influence of the constant force and the location of the vibration resonances – the natural frequencies for individual vibration modes. The study's main objective is to assess the possibility of emergency changing the manufacturing technology of selected machine components. The authors were interested in partially replacing costly and not environmentally friendly milling with 3D printing. Machine elements can be manufactured by printing in classical machine building and emergency conditions to replace a damaged component temporarily (e.g., on a ship, for the time of arrival at a port or shipyard). The main assumption guiding the authors during the preparation of this publication was the analysis of the possibility of using the production of “ad hoc” prepared spare parts and their use in the event of a lack of access to parts made of the intended materials.

**Keywords:** modal analysis, cavity method, additive method, machine element repair

### INTRODUCTIONS

Among the commonly used technologies for manufacturing machine components, machining methods (turning and milling) play the most important role, particularly in using CNC machine tools. Among the most important advantages of these machines, which determine their almost growing popularity, are their versatility and accuracy. CNC machine tools enable the creation of a series of elements with repeatability and allow the machining of a whole range of engineering

materials, from ferrous and non-ferrous alloys, through plastics and engineering ceramics to wood. It is often impossible to produce a workpiece using machining, especially when a complex geometric structure has been decided upon when designing the component. During cavity machining, the execution of deep pockets, transitions with sharp angles or corners with small radius of rounding may cause specific technological problems. In such cases, the technologist may decide to simplify the model by, adapting its geometry to the functionality of the existing

machinery and tools. The above aspects may have a decisive impact on the extension of the manufacturing process of machine elements and the final manufacturing costs of specific components [1–4]. Precise numerical machine tools are often unavailable and their operation requires high operator qualifications. In addition, there are places where the timely delivery of spare parts encounters many problems.

3D printers are relatively easy to use and have a small size. Unfortunately, the quality of the prints obtained from them and their technical parameters usually differ from the elements made on CNC machines. However, in situations where insignificant elements are damaged, it seems possible to temporarily replace them with 3D prints prepared on the spot. The authors intentionally compare the parameters of various materials to verify the impact of their use on one of the important parameters, which are the modes of natural vibrations.

When milling elements with complex shapes, the greatest efficiency is achieved by using multi-spindle machining centers and four or five-axis machine tools. The fundamental disadvantages of CNC machines include the high purchase price and high operating costs [5]. However, CNC machines allow cutting components with a more complex geometry than the three-axis milling machines often used. Milling with three-axis machine tools allow cutting only one surface and four sidewalls. The development of milling machines allows for complete processing of blanks in one clamping by increasing the number of controlled axes. Additional axes can be obtained by controlling headstock turning, table rotation or tilting the table (Figure 1). Four-axis CNC machines already allow simultaneous or indexed machining, which allows a maximum of four faces and one sidewall to be cut.

On the other hand, during machining with five-axis milling machines, indexed and simultaneous

machining is possible from five surfaces of the workpiece [2–4,7,8]. Limited possibilities of numerically controlled milling machines resulting from their kinematics, including five-axis machines, often necessitate using two or more fixtures during one milling operation. Each change of the element mounting, and even the change of tools during one operation, may lead to errors related to their basing and positioning. The above errors may result in the finished product exceeding permissible dimensional deviations [1,2,4,9].

The programming multi-axis numerically controlled machines, which are intended in particular for machining elements with complex geometry, require [2,4,5,9,10]:

- use of CAD design support software;
- use of CAM manufacturing software;
- having qualified staff with knowledge of the correct selection of machining parameters (i.e., cutting speed, recommended feeds, cutting layer depth, cutting layer width) and the specificity of the behavior of individual engineering materials during cutting;
- having staff with experience in the manufacturing process of machine and device components.

In applications such as rapid prototyping of machine components or emergency manufacture of temporarily unavailable spare parts, machining can be replaced by additive 3D printing. By 3D printing, we mean the process of physically producing objects by applying the build material layer by layer and selectively bonding it together. Currently, there are many methods of additive manufacturing.

Each 3D printing technique uses a different type of material that is bonded in another way. The work uses the method of thermoplastic filament extrusion – Figure 2, which is one of the world’s cheapest and most commonly used 3D printing techniques [12–15]. This technique is

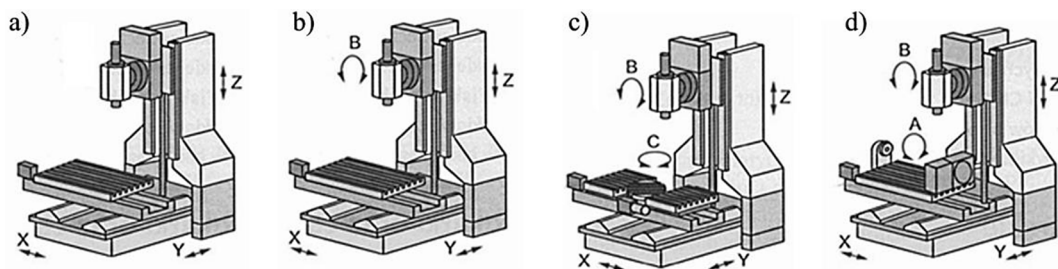
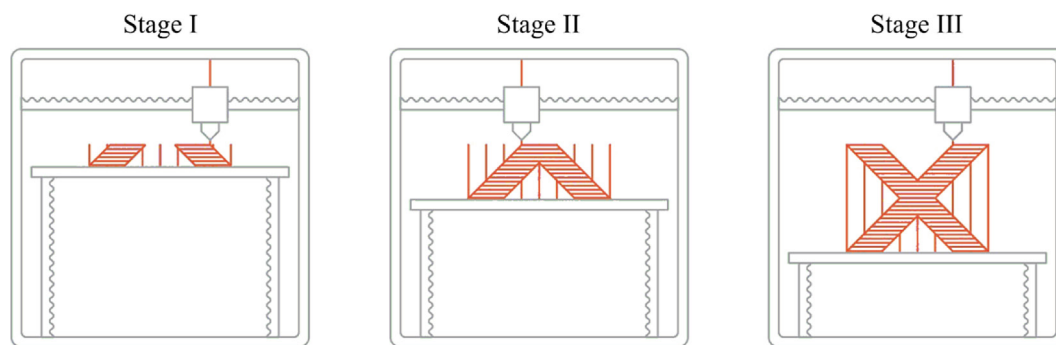


Fig. 1. The system of numerically controlled axes for milling machines: a) three-axis, b) four-axis, c) five-axis, d) five-axis [6]



**Fig. 2.** Stages of 3D printing in the FDM/FFF technique [11]

called Fused Deposition Modelling (FDM) or Fused Filament Fabrication (FFF) in the literature. For this study, the authors used the acronym FDM/FFF.

The FDM/FFF 3D printing technique uses thermoplastic filament. It may be in the form of polylactide (PLA) [16], acrylonitrile-butadiene-styrene terpolymer (ABS), poly-ethylene terephthalate (PET) or enriched with glycol PET known as PET-G, also thermoplastic polyurethane elastomer (TPU) is used as the build material [17–19]. The printing process is initiated in the head, where the material fed from the spool is melted into a semi-liquid form. Then the filament is directly extruded onto the printer's worktop. The material is only applied along a defined path along the X and Y axes. Once the material is applied in the XY plane in a given layer, the head with the nozzle moves along the Z axis by a preset value corresponding to the thickness of the layer. The material is then reapplied in only two axes (Figure 2). After application, the semi-fluid material cools down and is fused with the previously applied material fibers – creating a solid model. 3D printing in the FDM/FFF technique allows to obtain components of machines and devices with a dimensional accuracy of  $\pm 0.5\%$  (lower limit  $\pm 0.5$  mm) when using desktop 3D printers or  $\pm 0.15\%$  (lower limit  $\pm 0.2$  mm) with the use of industrial 3D printers [11,12,20,21]. This additive method enables free positioning of the printed detail in relation to the printing machine table. In incremental techniques, this is possible through the use of support material. It helps model to retain its shape, maintaining the dimensions of holes, indentations or overhangs of the solid. Cavity machining does not allow complex structures to be obtained, as is the case when 3D printing layer by layer, uses removable bases called supports [9,11,20]. When industrial 3D printers are used, the supports are generated almost in parallel with

the detail, usually using an additional print head. Depending on the filament type used, they can be later broken off the element or dissolved in a dedicated solution [11,20].

On the other hand, with desktop 3D printers, a single print head is usually used to create a support structure from the same filament as the element to be manufactured, but usually with a lower fill rate [11]. However, such generated support can significantly extend the printing process [9,22]. Details printed in the FDM/FFF technique can be subjected to additional finishing treatments. The basic postprocessing procedures include the removal of possible supports and obtaining a smoother model surface by treating the characteristic joining lines of the material layers [11,13,23–25].

3D printing in the FDM/FFF technique makes it possible to print high-quality and fully functional prototypes, demonstration models, and machine and equipment parts relatively quickly. The advantages of this technique include the possibility [11,20]:

- execution of production orders in a short period due to the high availability of FDM/FFF systems and a relatively short construction time of components;
- production of details from high-strength thermoplastics, including those that are resistant to high temperatures and also resistant to chemicals;
- use of various types of thermoplastic filament to produce high-quality functional prototypes and conceptual models, as well as components of machines and devices;
- use of a filament with a wide color gamut;
- printing of elements with relatively high dimensional and shape accuracy of  $\pm 0.15$  to  $\pm 0.3$  mm, depending on the complexity of the detailed geometry and the way it is arranged on the worktop;

- relatively fast printing of machine elements and devices with low material losses;
- use of a soluble support material;
- use of a 3D printer in the office or on board of a ship (so-called low-budget or desktop printers).

Among the most significant disadvantages of 3D printing using the FDM/FFF technique is the limited resistance of the elements made to mechanical loads causing a complex state of stress. It is related to the anisotropic nature of elements printed using this technique. The strength of these elements, when loaded with forces acting in the Z-axis direction is significantly lower than their strength in the case of loads acting in the XY plane [11,20,23].

3D printing technology and production with numerically controlled machine tools require dedicated CAD/CAM software. The 3D printing technology does not require as much specialized knowledge and experience as CNC machine programming. The operation of a 3D printer also does not require continuous calibration of the machine, thus not forcing constant operator involvement. The operation of 3D printers, especially desktop printers, is intuitive, and many printing parameters are generated automatically by the CAM programme. The work of the printer operator ends at the start of the printing process and only requires controlling the correctness of the printout. The situation is different in the case of work on a CNC machine tool, where the operator must constantly control the machining process and, if necessary, change the workpiece clamping [9,11].

Many scientific and industrial centers conduct research on the improvement of 3D printing technology [12, 13, 26–29]. Researches are conducted on a large scale in the field of determining the strength of new filaments, but they mainly relate to tests on tensile machines [30]. It is possible to find publications where dynamic characteristics of 3D printouts are examined, but only in relation to normalized samples [23]. The authors therefore attempted to compare the dynamic characteristics of an element made of steel (a material often used for the production of the tested elements) with geometrically similar replacement elements made in various 3D printing technologies.

## PURPOSE, SUBJECT AND METHODOLOGY OF RESEARCH

The study's main objective was to analyze the possibilities and determine the possibilities

of changing the emergency manufacturing technology of machine and equipment elements. The authors of the study compared the possibility of using alternative techniques for producing mechanical elements with the costly and non-ecological milling performed with numerically controlled machines. According to the authors, alternative techniques for producing machine elements are using an additive method in the form of 3D printing in the FDM/FFF technique. The choice of these two technologies for the research considerations was dictated by the fact that, they allow machine elements to be manufactured both under industrial conditions and in emergencies, such as for the temporary replacement of a damaged component on a ship during a voyage.

The subject of the experimental part of the research is a holder bracket made in accordance with Figure 3. This part is originally manufactured from C35 non-alloy structural steel by processing at a CNC machining center. The milling machine used during machining was Feeler NB-1300. For the tests, batches of samples were made that were in accordance with the dimensions of the original part drawing. Different technologies were used to make the elements than those in the original technical documentation. The samples were therefore made using the following methods:

- milling in three fixtures on a three-axis CNC milling machine from a steel blank (C35 steel) measuring  $108 \times 50 \times 50$  mm;
- incremental, using the FDM/FFF technique on an industrial printer from a thermoplastic filament in the form of polylactide – PLA (Table 1);

The prints were made on the Creatbot Peek 300 industrial 3D printer. As a slicer software the Ultimaker Cura 3D was used. Number of top and bottom layers were four and their height was 0.2 mm per layer.

The process of fabricating the samples by cavity machining included:

- making the spatial model – the finished element, in Autodesk Inventor and Solid Edge 2019;
- development of programs, “machining” for a three-axis CNC milling machine in EdgeCAM software, enabling the detail to be made in three fixtures;
- fabrication of elements in C35 steel on a three-axis CNC milling machine in three fixtures (Figure 4).

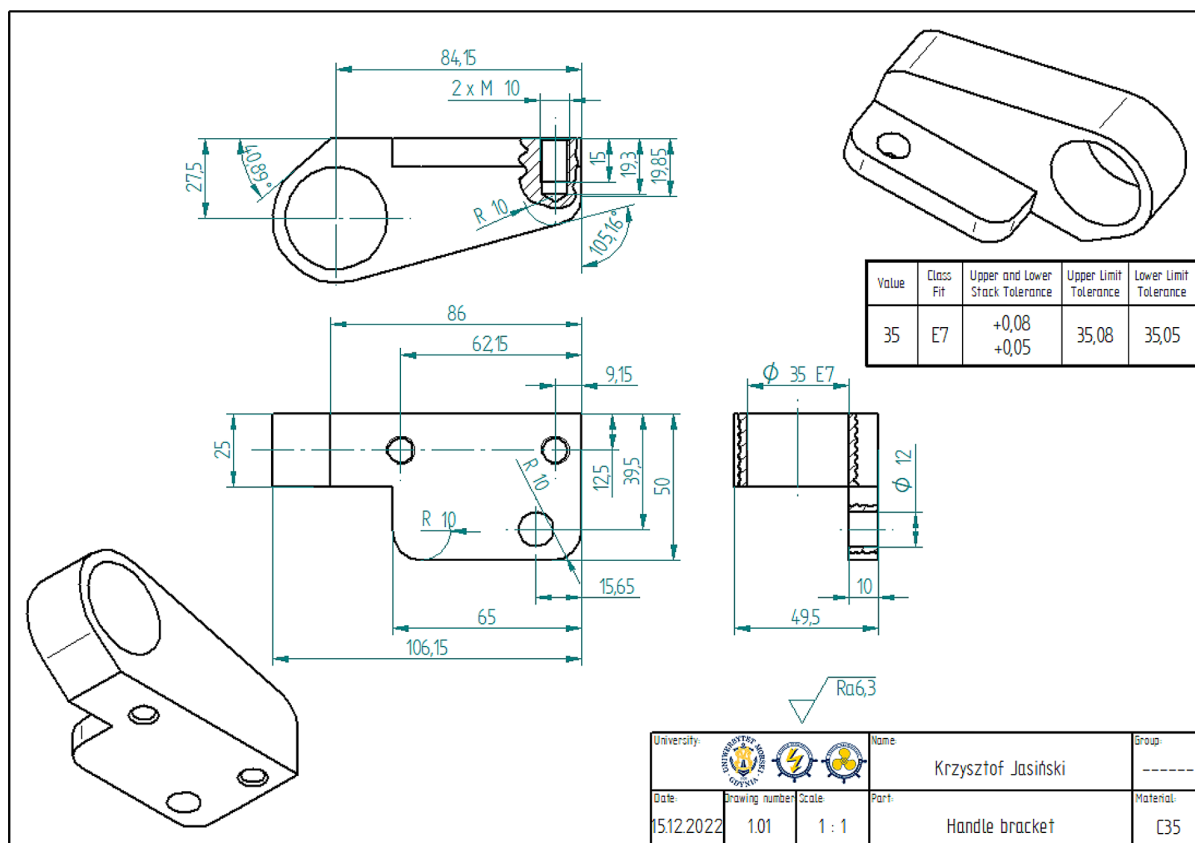


Fig. 3. Technical drawing of the holder bracket /own development/.

The process of manufacturing samples using the incremental FDM/FFF technique included:

- making the spatial model – the finished element, in Autodesk Inventor and Solid Edge 2019;

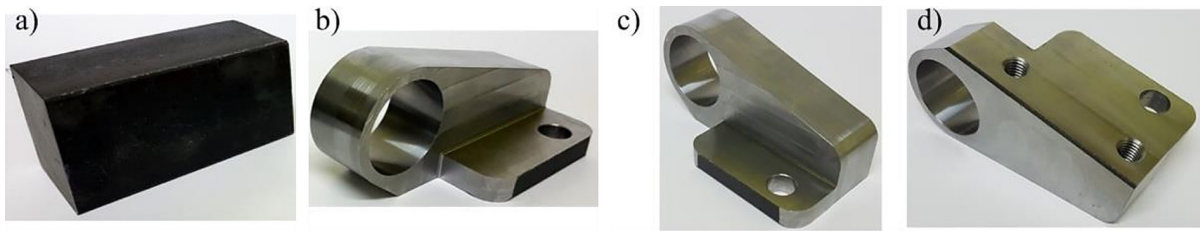
- development of print programmes using Ultimaker Cura 3D software taking into account different filling levels (10%, 20%, 50%, 100%);
- printing the workpieces on a 3D printer with varying fill levels (Figure 5). A brass nozzle with a diameter of  $\varnothing 0.4$  mm was used to print the details from PLA filament using the FDM/FFF technique.

Table 1. Properties and parameters of the filaments used /own elaboration/

Parameter / Property	Filament PLA 
Filament diameter [mm]	1.75 ± 0.03
Heat Distortion Temperature [°C]	45 ÷ 65
Recommended printing nozzle temperature [°C]	200 ÷ 220
Recommended 3D printer table temperature [°C]	0 ÷ 60
Recommended printing speed [mm/s]	50 ÷ 90
Density [g/cm <sup>3</sup> ]	1.3
Yield strength [MPa]	45
Modulus of longitudinal elasticity [MPa]	2000
Elongation at break [%]	2.5
Process shrinkage [%]	0.4

The temperature of the printing nozzle (205°C) and the temperature of the printer table (45°C) were rigorously controlled to ensure the reproducibility of the mechanical properties of the printed elements. Currently, there are about ten 3D printing techniques elements with the specified filling.

During printing, the room temperature and air humidity were kept constant at 20°C and 55%, respectively. The print parameters resulting from the material used (printing nozzle temperature, printer bed temperature, room temperature and air humidity, intensity of cooling – or lack of it) were set in accordance with the recommendations of the filament manufacturer. The print parameters related to the functional features of the 3D printers used (feed,



**Fig. 4.** Sample made using the cavity method /own development/

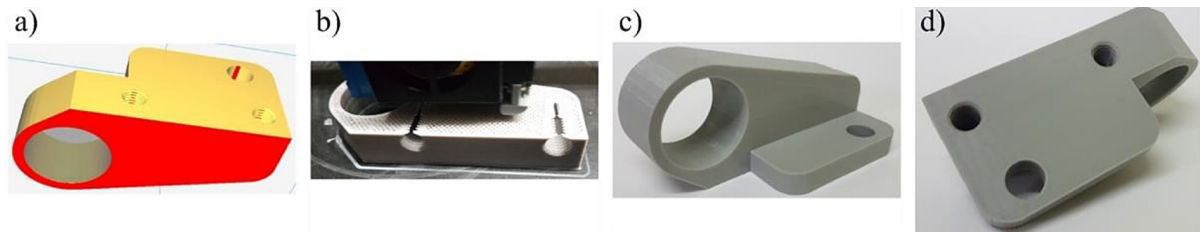


**Fig. 5.** Sample with a 20% filling made using FDM/FFF technique: a) analysis of overhanging surfaces in Ultimaker Cura 3D software, b) printout of overhangs in the threaded holes of the model, c) view of the workpiece after printing from the front, d) view of the workpiece after printing from below /own elaboration/

machine passes) were selected based on the operator’s experience and suggestions implied in the Ultimaker Cura software. If the process of printing the sample layer was not correct, the printout was ended and it was repeated from the beginning by introducing the necessary adjustments to the settings of the appropriate parameters.

To achieve the objective of the work, a research programme was carried out, which included:

- a comprehensive technical analysis of the production of the holder bracket using the technologies discussed;
- determination of resonance curves, i.e., the level of vibration amplitudes depending on the excitation frequency while maintaining a constant force generated by the exciter, of steel samples and samples printed using the FDM/FFF technique (at different filling levels).

## TECHNICAL ANALYSIS THE HOLDER BRACKET PRODUCING METHODS

An analysis was carried out on the manufacturing process of the holder bracket using:

- samples made traditionally by machining (cavity method) – Figure 11a);
- samples made using 3D printing using the FDM/FFF technique with a filling of 50% – figure 6b and filling of 20% – Figure 6c);

The conducted analysis included:

- evaluation of the process flow of sample fabrication by individual technologies (Table 2 and Table 4);
- determination of sample production times by individual technologies (Table 3);
- assessment of the structure of the control programmes used during sample production by individual technologies;

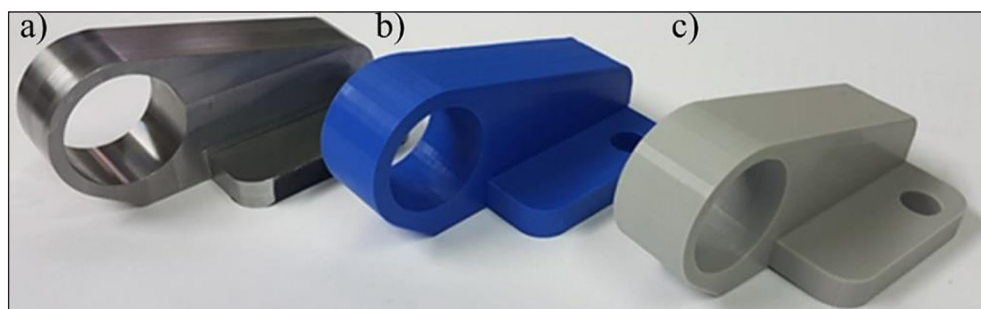


**Fig. 6.** Samples used during the technical and economic analysis: a) detail made using the cavity method, b-c) detail made using the additive method

**Table 2.** Comparative analysis of the sample production process /own elaboration/.

Type of manufacturing means	Type of manufacturing method	
	Cavity	Incremental
Machine	CNC milling machine	3D printer
Fixing	Machine vice	Mat
Material	Steel C35	PLA filament
Cooling	Emulsion	Air
Tools	ø32 milling head with plates for steel VHM milling cutter ø14 z4 – rough VHM milling cutter ø10 z4 VHM milling cutter ø20 z4 ø22 drill VHM drill bit ø12 VHM drill bit ø8.5 HSCO chamfer cutter ø12 M10x1.5 torsional machine tap boring bar ø35	Printing nozzle ø0.4mm

- determination of the purchase costs of the monolithic tools required to produce samples by individual technologies (Table 4).

The results of the analysis are presented synthetically in Tables 2–4.

Each of the methods presented made it possible to produce samples according to the dimensional criteria set. The cavity method, using a numerically controlled machine, is characterized by high accuracy of the manufactured element and little need for additional detail processing after removal from the machine. Achieving such a result, however, requires the use of a number of production means that not only take part in the processing of the element but also support auxiliary processes (e.g., 3D edge sensor).

A CNC machine tool requires a dedicated machining programme generated using paid CAM software. Operating a programme such as EdgeCAM requires skilled personnel capable of using its capabilities. Making a detail from a cubic blank resulted in up to 66% material losses. Manufacturing with such a material loss can be a

source of waste disposal problems. The machining process itself is a rather onerous process for the operator due to: noise, vibration, and fumes from emulsions and oils. It also has a negative impact on the human body.

In the case of the incremental method based on 3D printing using the FMD/FFF technique, the production stage itself required only PLA filament, a suitable printing nozzle with a diameter of ø4 mm and strict control of the basic parameters, i.e., nozzle temperature of 205°C, work table temperature of 45°C, the amount of material fed by the extruder to the printer nozzle, the print speed, as well as the efficiency of fans cooling the created detail. Unfortunately, the resulting model was not as accurate as when using the cavity method and required additional postprocessing, in the form of correcting the ø35 mm hole diameter with a hand reamer and correcting the M10 x 1.5 threads with a hand tapping tool (table 4). Preparing a programme for a 3D printer is not as complicated a process as preparing a programme for a CNC machine tool. In addition, 3D printing makes it possible to produce a detail

**Table 3.** Comparative analysis of the sample production time /own elaboration/

Time	Type of manufacturing method				
	Cavity			Incremental	Incremental
					
	Assembly 1	Assembly 2	Assembly 3	3D print – 50% infill level	3D print – 20% infill level
Operation time	5.7 minutes	5.7 minutes	5.8 minutes	194 minutes	139 minutes
Total time	17 minutes			194 minutes	139 minutes

**Table 4.** Comparative analysis of production methods /own elaboration/

Parameter analyzed	Type of manufacturing method	
	Cavity 	Incremental 
Accuracy of execution	High	Low
Execution time	Short	Long
Time required to prepare programmes and machines	Long	Brief
Waste of material	66%	Negligible
Number of tools	11	1
Cost of cutting tools	280 Euro	Not applicable
Possible additional activities (postprocessing)	Trimming	Improvement of M10 threads reaming the hole ø35

from a single control programme, which significantly simplifies the production process itself and, at the same time, eliminates the possibility of various types of inaccuracies that arise from changes in the fixture of the workpiece. Additive production reduces the loss of print material to practically zero (Table 4). In some cases, it even allows it to be saved. This is possible by making the created detail with partial filling.

**Holder bracket dynamic characteristics**

In addition to the previously assessed characteristics of the holder, such as accuracy of workmanship, material loss, production time and possible costs, as well as strength, it is extremely important to analyze the dynamic properties of the tested element. The most effective way to assess the dynamics of a structure is to determine its resonance curve, i.e., the level of vibration amplitudes as a function of the excitation frequency, assuming a constant excitation magnitude [23,31–35]. The vibration magnification coefficients are of interest, defined as the ratio of the vibration amplitudes in resonance to the static deformation under an invariant force. More important, however, is the position of the vibration resonances – the natural frequencies for the different forms of natural vibration [32,33,36]. The natural frequencies are proportional (equal for a system with one degree of freedom) to the stiffness of the tested element. Both mass and stiffness of machine parts are often overlooked when analyzing the kinematics and dynamics of machine operation and are undoubtedly very important due to their typical process. Structural stiffness is a complex issue, as one can consider stiffness changes in different directions

and analyze coupled stiffnesses or stiffness changes under the influence of load, temperature, vibration frequency, etc. [31,37–39]. The authors used a single parameter, defined according to relation (Eq. 1), to assess stiffness.

$$k_i \cong \omega_{Ni}^2 \cdot m \tag{1}$$

where:  $k_i$  – generalized stiffnesses of the structure;  
 $\omega_{Ni}$  – natural frequencies for the i-th form;  
 $m$  – mass of the component under test.

To determine the resonance curves of the holder bracket a Bruel & Kjaer type V555 vibration exciter was used together with appropriately mounted piezoelectric vibration sensors. It allows to conduct experimental modal analysis (EMA). All holder brackets were fixed identically. The asymmetrical mounting enables a relatively large number of tested holder natural vibration modes to be excited. Pictures of selected components of the measurement system and the method of mounting the cantilever holder and piezoelectric sensors are shown in Figure 7.

EMA is a process consisting in the experimental determination of the resonance frequencies of the tested system. With the use of appropriate techniques, it is also possible to determine the mode of natural vibrations. EMA has many advantages as it is a fast, relatively cheap and simple method of determining resonance frequencies. The output equation for modal analysis is the general equation of the oscillating motion:

$$m\ddot{x}(t) + c\dot{x}(t) + kx(t) = f(t) \tag{2}$$

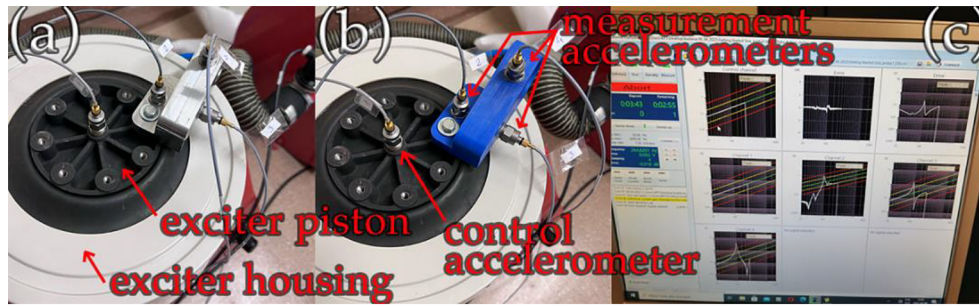


**Fig. 7.** Dynamic test course – mounting of piezoelectric sensors and the holder bracket on the vibration exciter: a) taking characteristics from the sample made of C35 steel, b) taking characteristics from the sample filled with 50% of filament, c) a screenshot with an image of the measurement programme – course of measurement curves /own elaboration/.

where:  $m$  – mass,  $c$  – damping ratio,  $k$  – elasticity coefficient.

Eq. 1 can be converted to the form

$$[-m\omega^2 + jc\omega + k]X(\omega) = F(\omega) \quad (3)$$

Considering that:

$$H(\omega) = \frac{1}{-m\omega^2 + jc\omega + k} \quad (4)$$

It can be written:

$$H(\omega) = \frac{X(\omega)}{F(\omega)} \quad (5)$$

$H(\omega)$  is known as FRF – frequency response function. The FRF describes the ratio of the Fourier transform at the output of the  $X(\omega)$  system to the Fourier transform of the forcing applied to the  $F(\omega)$  system.

The exciter piston moved with a constant acceleration amplitude of 1.5 g in the range: 10–6000 Hz, the rate of frequency change (sweep rate) – 1 oct/min. The error of the piston movement in relation to the set parameters was negligible. An example of a diagram of piston acceleration amplitudes (dynamic forcing) recorded during testing of a metal cantilever is shown in Figure 8. Each test was carried out three times to determine some of the measurement errors. The dispersion of the measurement results did not exceed 0.5%.

Tests were carried out on cantilever samples made from C35 steel using the cavity method and on four types of models of this component made

using the additive method from PLA filament with different filling levels. In order to facilitate subsequent identification of the samples, which were produced using the incremental method, filaments of different colours were used during printing, depending on the adopted filling degree of the workpiece. The influence of dyes on the properties of the filament was treated as negligibly small. Parameters characterizing the samples and simulations of the longitudinal sections of the elements obtained by FMD/FFF printing are shown in Table 5 and Figure 9. Table 6 presents the results of samples geometry verification conducted with Artec Leo 3D scanner. Scanned geometry was compared to initial geometry from the project.

Considering the dynamics of the structure, both the stiffness is determined according to the direction of action of the forcing (in this case, these are the data collected with measurement channel No. 4) and the coupled stiffness (based on data from measurement channel No. 3) are of interest. An example of the resonance curve determined for a steel cantilever based on data from channel No. 4 is shown in Figure 10, while Figure 11 shows the resonance curve of a steel cantilever obtained from the results of channel No. 3 (which recorded measurement data in the direction perpendicular to the direction of dynamic forcing). As expected, the accuracy of the determination of the resonance curve in the direction perpendicular to the direction of action of the forcing is reduced for low frequencies (noise in the range of 10–50 Hz is observable in Figure 11. However, this noise does not affect the analytical value of the results obtained, as all natural frequencies determined for the tested holder brackets were observed above 100 Hz.

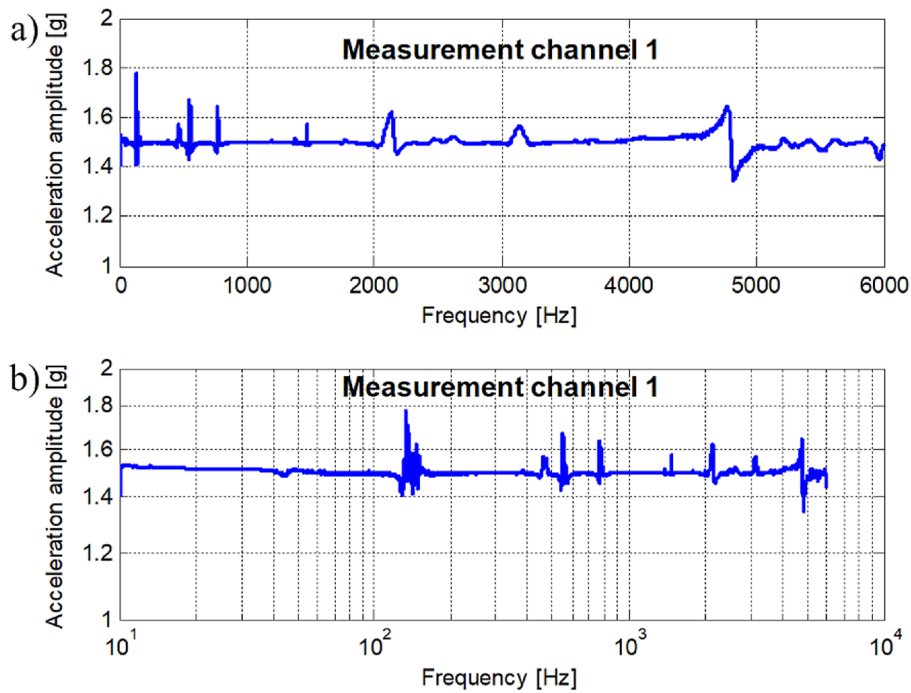


**Fig. 8.** Amplitudes of vibration accelerations of dynamic excitation: a) graph on linear scale, b) graph on logarithmic scale /own elaboration/.

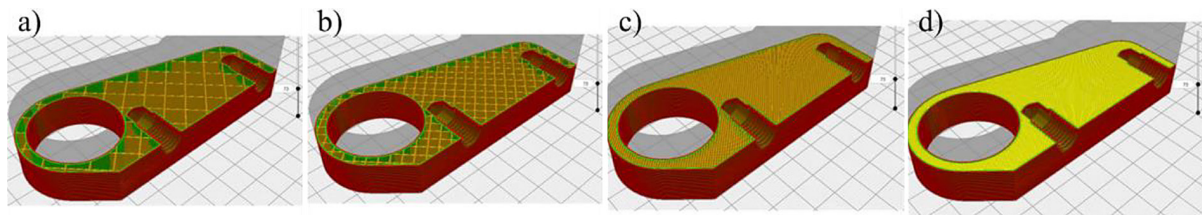


**Fig. 9.** Simulations of the longitudinal cross-section of holder bracket samples when printed in the FDM/FFF technique depending on the degree of filling: a) 10% filling, b) 20% filling, c) 50% filling, b) 100% filling /own elaboration/.

The holder bracket under consideration is a compact component and, as expected, its vibration magnification factor does not exceed a value of 7 for the detail made of C35 steel and the samples made of PLA filament with different filling levels.

The values of the vibration amplitudes at resonance (which are most dangerous in terms of structural dynamics) will, therefore not differ significantly for the cantilevers under consideration, regardless of whether the samples used were

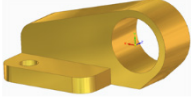
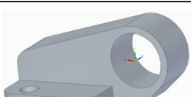
made of C35 steel or PLA filament with different filling levels. On the other hand, clear differences were observed in the position of the natural resonance frequencies of these cantilevers. Figure 12 and Figure 13 show summary plots of the resonance curves for all the samples analyzed.

In both analyzed directions, three main forms of natural vibration and their corresponding natural frequencies can be distinguished. The natural frequencies for the individual holder bracket samples are shown in Table 7 and Table 8. By

**Table 5.** Samples 3D scanning results compared to CAD project

Material and fill level	Steel 100%	Golden 100%	Blue 50%	Gray 20%	White 10%
3D Scanning view					
Root mean square of shape deviations [mm]	0.2111	0.1482	0.2519	0.1432	0.1526

**Table 6.** Parameters characterizing the samples subjected to dynamic tests /own elaboration/.

Sample model	Color of sample	Manufacturing method	Material	Fill level	Processing time	Sample weight
	Steel	Cavity	Steel C35	100%	17.4 minutes	697 g
	Golden	Additive	Filament PLA	100%	624 minutes	99 g
	Blue	Additive	Filament PLA	50%	194 minutes	58 g
	Gray	Additive	Filament PLA	20%	139 minutes	50 g
	White	Additive	Filament PLA	10%	117 minutes	41 g

comparing the resonance curves shown in Figures 12 and 13 and the identified natural frequencies shown in Tables 6 and 7, correlations between the vibration-diagnostic test results obtained in the two mutually perpendicular directions are noted. In the low-frequency band (i.e., 10 – 50 Hz), a strong noisiness can be observed in the characteristics of Figure 13 but already for higher frequencies, the resonance curves of the cantilevers are similar in terms of natural frequencies in both directions. In contrast, the

observed acceleration amplitudes are about 50 % larger for the direction in line with the direction of the dynamic forcing. Thus, both piezoelectric accelerometers recorded the same, i.e., torsional forms of natural vibration. Uncoupled forms of vibration, i.e., only vertical or only horizontal vibrations, are imperceptible. This observation is consistent with the assumptions made in the research, which sought to reduce the influence of boundary conditions as much as possible. For this reason, the mounting of the samples on the

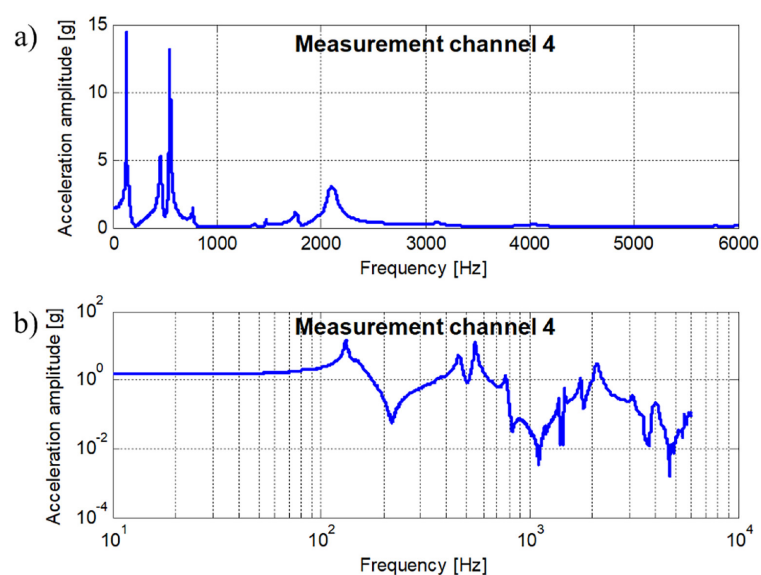


**Fig. 10.** Resonance curve for a steel cantilever measured in the direction of the dynamic excitation: a) graph on a linear scale, b) graph on a logarithmic scale /own elaboration/

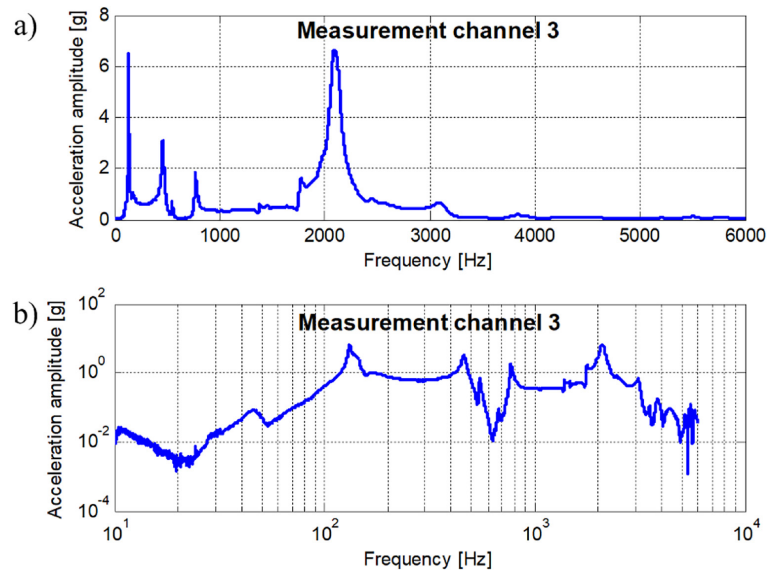


**Fig. 11.** Resonance curve for a steel cantilever measured perpendicular to the direction of the dynamic forcing: a) linear scale plot, b) logarithmic scale plot /own elaboration/

piston of the exciter (see Figure 7) was used, as it also allows torsional forms of natural vibration to be recorded – if present, of course. Therefore, in the following, the test results obtained only from measurement channel 4, which provided data measured in the direction consistent with the direction of the dynamic excitation, were analyzed.

The identified natural frequencies for the cantilever made from C35 steel differ markedly from those of the samples made from PLA filament. A correlation was also observed between

the natural frequencies of cantilevers made using the additive method and the degree of filament filling. One reason for the different distribution of natural frequencies for this group of cantilevers is the significant difference between the masses of cantilevers made using the cavity method and samples printed using the FMD/FFF technique (additive method). However, in the case of components made using the incremental method with different internal filling, the distribution of natural frequencies depends not only on the mass of the samples but also on the uniform distribution

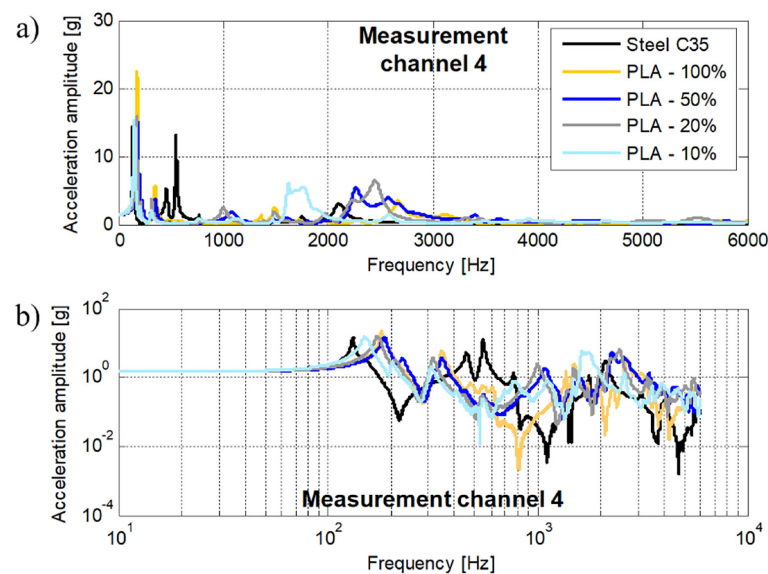


**Fig. 12.** Resonance curves for the holder brackets measured in the direction consistent with the direction of the dynamic forcing: a) graph on a linear scale, b) graph on a logarithmic scale /own work/

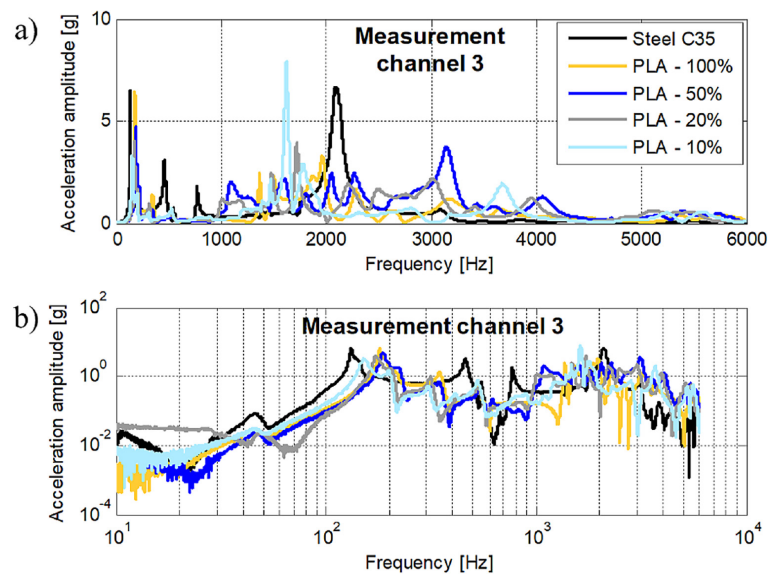


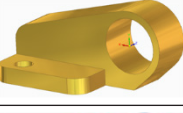
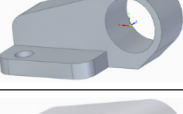
**Fig. 13.** Resonance curves for the holder brackets measured perpendicular to the direction of the dynamic forcing: a) graph on a linear scale, b) graph on a logarithmic scale /own elaboration/

of the filament in the volume of the test samples. In the operation of mechanical components, however, the most important factor is their dynamic stiffness, broken down into various forms of vibration. Table 8 summarizes the stiffnesses, which were determined according to relation (Eq. 1) (including units of measure).

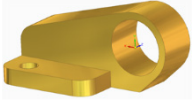
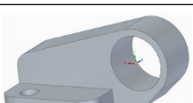
The stiffness of a steel cantilever that is made using the classic cavity method with a CNC

milling machine is many times that of a cantilever made with a 3D printer using the FMD/FFF technique. For the most important, i.e., the first form of vibration, the stiffness of the steel cantilever is four times greater than that of a cantilever made from 100 % filled filament (gold-colored element in Table 9). At higher excitation frequencies, the situation only worsens. The fabrication of machine components with 3D printers using

**Table 8.** Main resonant (natural) vibration frequencies identified perpendicular to the direction of dynamic forcing /own elaboration/

Sample model	Color of sample	Manufacturing method	Material	Fill level	Natural frequency [Hz]		
					Resonance zone number		
					1	2	3
	Steel	Cavity	Steel C35	100%	132.045	458.31	2096.45
	Golden	Additive	Filament PLA	100%	179.477	345.721	2612.92
	Blue	Additive	Filament PLA	50%	185.969	345.316	2266.73
	Gray	Additive	Filament PLA	20%	171.262	313.446	2487.48
	White	Additive	Filament PLA	10%	150.733	306.786	1618.92

**Table 9.** Summary of dynamic stiffnesses of individual brackets, taking into account the form of vibrations determined in the direction consistent with the direction of the dynamic excitation /own elaboration/

Sample model	Color of sample	Manufacturing method	Material	Fill level	Dynamic stiffness [N/m]		
					Vibration form number		
					1	2	3
	Steel	Cavity	Steel C35	100%	$4.80 \times 10^5$	$57.62 \times 10^5$	$12.20 \times 10^7$
	Golden	Additive	Filament PLA	100%	$1.26 \times 10^5$	$4.73 \times 10^5$	$2.78 \times 10^7$
	Blue	Additive	Filament PLA	50%	$0.79 \times 10^5$	$2.78 \times 10^5$	$1.17 \times 10^7$
	Gray	Additive	Filament PLA	20%	$0.57 \times 10^5$	$1.98 \times 10^5$	$1.18 \times 10^7$
	White	Additive	Filament PLA	10%	$0.36 \times 10^5$	$1.56 \times 10^5$	$0.43 \times 10^7$

the FDM/FFF technique should be limited to emergencies if we make them using the one-to-one method. If we want to apply a new manufacturing technology, we should consider this fact already in the design phase. Nevertheless, 3D printing seems to be a very interesting technology to use in emergency situations. Particularly on ships, the workshop equipment should include a 3D printer to enable the ship to arrive in port as smoothly as possible. In this case, products with 100 % filament fill should be used. Saving on fill allows a maximum gain of two and a half times the weight, with a further reduction in dynamic stiffness of almost four times. Of course, there are printers using better materials (e.g., metal alloys), but these are far more expensive and less obvious as emergency equipment (e.g., on a ship).

**CONCLUSIONS**

The results presented in Tables 7 and 8 confirm the theoretical assumptions about the increase in the frequency of individual modes of free vibrations and the decrease in the mass of individual tested samples. It should be emphasized, however, that the value of the stiffness of dynamic samples decreases along with the degree of filling in subsequent 3D prints – Table 9. From

the point of view of time and costs, The most economical is a printout with the least 10% fill ratio (Table 6), however, it can only be used temporarily for structures with little load. From the point of view of possibly high dynamic stiffness, it is advisable to use printed elements with the greatest possible filling. The printing time is less important here because after selecting the appropriate settings, the printer works automatically.

The authors of the study believe that the additive method realized in the form of 3D printing in the FDM/FFF technique can provide an interesting alternative for the manufacture of a spare part in an emergency situation. This is confirmed by both the results of the technical and economic analysis developed for the case of manufacturing a holder bracket and the dynamic characteristics of the components tested. On the basis of the research described above, the authors believe that investigation into the possibility of using these production methods in the emergency manufacture of spare parts for repairs during ship voyages should be continued. Further research tasks should include the determination of new dynamic characteristics for the holder brackets and the performance of strength tests.

The authors plan to conduct dynamic tests to determine the dynamic stiffness, using samples with varying degrees of filling made with other

filaments like ABS filament. However, in this case, the strength tests should consist of a static tensile test and a static torsion test for standard samples ( $d = 10 \text{ mm}$ ,  $l = 10 d$ ) with varying degrees of filling. As in the case of the holder bracket samples, the standard samples should be obtained by the incremental method from PLA filament and ABS filament. The determination of the individual strength limits, particularly the longitudinal elastic modulus  $E$  and the modulus of formability  $G$ , will allow the strength of the correlation between the dynamic and strength tests to be determined.

## REFERENCES

- Feld M. Podstawy projektowania procesów technologicznych typowych części maszyn, 5th ed.; Wydawnictwo Naukowe PWN, 2022.
- Cichosz P. Nowoczesne procesy obróbki skrawaniem, 1st ed. Wydawnictwo Naukowe PWN, 2022.
- Raj R., Dixit A.R., Łukaszewski K., Wichniarek R., Rybarczyk J., Kuczko W., Górski F. Numerical and Experimental Mechanical Analysis of Additively Manufactured Ankle–Foot Orthoses. *Materials* 2022; 15(17): 6130. <https://doi.org/10.3390/ma15176130>
- Abas M., Habib T., Noor S., Salah B., Zimon D. Parametric Investigation and Optimization to Study the Effect of Process Parameters on the Dimensional Deviation of Fused Deposition Modeling of 3D Printed Parts. *Polymers* 2022; 14(17): 3667. <https://doi.org/10.3390/polym14173667>
- Silva F.J.G., Sousa V.F.C., Pinto A.G., Ferreira L.P., Pereira T. Build-Up an Economical Tool for Machining Operations Cost Estimation. *Metals* 2022; 12(7): 1205.
- Information on <http://www.avia.com.pl>.
- Olszak W. Obróbka skrawaniem, 1st ed.; Wydawnictwo Naukowe PWN, 2022.
- Grzesik W. Podstawy skrawania materiałów konstrukcyjnych, 3rd ed.; Wydawnictwo Naukowe PWN, 2018.
- Wierzchowski J. Porównanie nowoczesnych metod wytwarzania części maszyn wraz z weryfikacją rzeczywistych efektów technicznych i ekonomicznych, ich zastosowania w produkcji jednostkowej i małoseryjnej, Engineering Thesis, University of Information Technology and Management in Olsztyn, 2021.
- Przybylski W., Deja M. Komputerowo wspomagane wytwarzanie maszyn, 3rd ed.; Wydawnictwo Naukowe Techniczne, 2007.
- Zieliński D. Drukowanie Trwałych Elementów z Tworzyw Termoplastycznych w Technologii FDM/FFF. *Tworzywa Sztuczne w Przemysle* 2021, 4, 103–106.
- Ramya A., Vanapalli S. 3d Printing Technologies In Various Applications. *International Journal of Mechanical Engineering and Technology* 2016; 7(3): 396–409: 14.
- Vijay S.A., Shakil M.S., Patil M.P.M. Rapid Manufacturing Process – 3D Printing Technology Advantages, Disadvantages and Applications 2016; 4(11):4.
- Murawski L. Modelowanie numeryczne konstrukcji i urządzeń okrętowych, wyd. 1, Uniwersytet Morski w Gdyni, 2020.
- Fico D., Rizzo D., De Carolis V., Montagna F., Esposito Corcione C. Sustainable Polymer Composites Manufacturing through 3D Printing Technologies by Using Recycled Polymer and Filler. *Polymers* 2022; 14(18): 3756. <https://doi.org/10.3390/polym14183756>
- Gunasekaran K.N., Aravinth V., Muthu Kumaran C.B., Madhankumar K., Pradeep Kumar S. Investigation of mechanical properties of PLA printed materials under varying infill density. *Materials Today: Proceedings* 2021; 45: 1849–56.
- Mercado-Colmenero J.M., Rubio-Paramio M.A., la Rubia-Garcia M.D., Lozano-Arjona D., Martín-Doñate C.A. Numerical and Experimental Study of the Compression Uniaxial Properties of PLA Manufactured with FDM Technology Based on Product Specifications. *Int J Adv Manuf Technol* 2019; 103(5): 1893–1909. <https://doi.org/10.1007/s00170-019-03626-0>
- Chacón J.M., Caminero M.A., García-Plaza E., Núñez P.J. Additive Manufacturing of PLA Structures Using Fused Deposition Modelling: Effect of Process Parameters on Mechanical Properties and Their Optimal Selection. *Materials & Design* 2017; 124: 143–157. <https://doi.org/10.1016/j.matdes.2017.03.065>
- Rodríguez J.F., Thomas J.P., Renaud J.E. Mechanical Behavior of Acrylonitrile Butadiene Styrene (ABS) Fused Deposition Materials. *Experimental Investigation. Rapid Prototyping Journal* 2001; 7(3): 148–158. <https://doi.org/10.1108/13552540110395547>
- Dodziuk H. Druk 3D/AM. Zastosowania oraz skutki społeczne i gospodarcze, 1st ed.; Wydawnictwo Naukowe PWN, 2019.
- Yao T., Deng Z., Zhang K., Li S. A Method to Predict the Ultimate Tensile Strength of 3D Printing Polylactic Acid (PLA) Materials with Different Printing Orientations. *Composites Part B: Engineering* 2019; 163: 393–402. <https://doi.org/10.1016/j.compositesb.2019.01.025>
- Veiga F., Bhujangrao T., Suárez A., Aldalur E.,

- Goenaga I., Gil-Hernandez D. Validation of the Mechanical Behavior of an Aeronautical Fixing Turret Produced by a Design for Additive Manufacturing (DfAM). *Polymers* 2022; 14: 2177. <https://doi.org/10.3390/polym14112177>
23. Kanna S., Ramamoorthy M. Mechanical characterization and experimental modal analysis of 3D Printed ABS, PC and PC-ABS materials. *Mater Res Express*. 2020; 7(1): 015341.
  24. Karimi A., Mole N., Pepelnjak T. Numerical Investigation of the Cycling Loading Behavior of 3D-Printed Poly-Lactic Acid (PLA) Cylindrical Lightweight Samples during Compression Testing. *Applied Sciences* 2022; 12(16): 8018. <https://doi.org/10.3390/app12168018>
  25. Ajao K.R., Ibitoye S.E., Adesiji A.D., Akinlabi E.T. Design and Construction of a Low-Cost-High-Accessibility 3D Printing Machine for Producing Plastic Components. *Journal of Composites Science* 2022; 6(9), 265. <https://doi.org/10.3390/jcs6090265>
  26. Sellami T., Jelassi S., Darcherif A.M., Berriri H., Mimouni M.F. Experimental validation of a numerical 3-D finite model applied to wind turbines design under vibration constraints. *Mechanics & Industry* 2017; 18(8): 806.
  27. Wei X., Behm I., Winkler T., Scharf S., Li X., Bähr R. Experimental Study on Metal Parts under Variable 3D Printing and Sintering Orientations Using Bronze/PLA Hybrid Filament Coupled with Fused Filament Fabrication. *Materials* 2022; 15(15): 5333.
  28. Wang X., Jiang M., Zhou Z., Gou J., Hui D. 3D printing of polymer matrix composites: A review and prospective. *Composites Part B: Engineering* 2017; 110: 442–58.
  29. Górski F., Wichniarek R., Kuczko W., Żukowska M., Suszek E. Rapid Manufacturing of Individualized Prosthetic Sockets. *Advances in Science and Technology Research Journal*. 2020; 14(1): 42–49. DOI: 10.12913/22998624/113425
  30. Dizon J.R.C., Espera A.H., Chen Q., Advincula R.C. Mechanical characterization of 3D-printed polymers, *Additive Manufacturing*, Volume 20, 2018, Pages 44–67, <https://doi.org/10.1016/j.addma.2017.12.002>.
  31. P. Lesage, L. Dembinski, R. Lachat, S. Roth, Mechanical Characterization of 3D Printed Samples under Vibration: Effect of Printing Orientation and Comparison with Subtractive Manufacturing. *Results in Engineering* 2022, 13, 100372. <https://doi.org/10.1016/j.rineng.2022.100372>.
  32. Z. Osiński, *Teoria drgań*, 1st ed.; Wydawnictwo Naukowe PWN, 1978.
  33. T. Uhl, *Komputerowo wspomaganą identyfikacją modeli konstrukcji mechanicznych*, 1st ed.; Wydawnictwo Naukowe Techniczne, 1997.
  34. C. van Zijl, K. Soal, R. Volkmar, Y. Govers, M. Böswald, A. Bekker, The use of operational modal analysis and mode tracking for insight into polar vessel operations. *Marine Structures*. 2021; 79:103043.
  35. W.A. Siswanto, M.N. Ibrahim, M.A. Madlan, S.M. Mohamad, Shaker Table Design for Electronic Device Vibration Test System. *IJET*. 2011;3(6):663–8.
  36. Á. Encalada-Dávila, L. Pardo, Y. Vidal, E. Terán, C. Tutivén, Conceptual Design of a Vibration Test System Based on a Wave Generator Channel for Lab-Scale Offshore Wind Turbine Jacket Foundations. *JMSE*. 2022;10(9):1247.
  37. W. Heylen, S. Lammens, P. Sas, *Modal Analysis Theory and Testing*, 1st Ed.; Katholieke Universiteit Leuven: Oude Markt 13 3000 Leuven, Leuven, 1997.
  38. B.T. Phillips, J. Alder, G. Bolan, R.S. Nagle, A. Redington, T. Hellebrekers, J. Borden, N. Pawlenko, S. Licht, Additive Manufacturing Aboard a Moving Vessel at Sea Using Passively Stabilized Stereolithography (SLA) 3D Printing. *Additive Manufacturing* 2020, 31, 100969. <https://doi.org/10.1016/j.addma.2019.100969>.
  39. L. Virgin, 3D-Printing and Vibration (Including Resonance). *The Journal of the Acoustical Society of America* 2018, 143 (3), 1817–1817. <https://doi.org/10.1121/1.5035963>.